

Copyright © 2001, by the author(s).  
All rights reserved.

Permission to make digital or hard copies of all or part of this work for personal or classroom use is granted without fee provided that copies are not made or distributed for profit or commercial advantage and that copies bear this notice and the full citation on the first page. To copy otherwise, to republish, to post on servers or to redistribute to lists, requires prior specific permission.

**MICROWAVE CAVITY PERTURBATION  
TECHNIQUES TO MEASURE ELECTRON  
DENSITY IN UNSTABLE PLASMAS**

by

Tobias Locsei

Memorandum No. UCB/ERL M01/4

22 January 2001

**MICROWAVE CAVITY PERTURBATION  
TECHNIQUES TO MEASURE ELECTRON  
DENSITY IN UNSTABLE PLASMAS**

by

Tobias Locsei

Memorandum No. UCB/ERL M01/4

22 January 2001

**ELECTRONICS RESEARCH LABORATORY**

College of Engineering  
University of California, Berkeley  
94720

**Abstract:**

Several microwave cavity perturbation methods have been explored with the aim of developing a technique to measure the electron density  $n_e$  in unstable, low-pressure, inductive processing discharges. Ultimately these techniques would be applied to a Transformer Coupled Plasma (TCP). Preliminary testing was done on a mercury vapor discharge tube plasma on the axis of a smaller cavity to assess the feasibility of various measurement systems. It was found that a single frequency system was more appropriate than swept frequency raster display with the available equipment. Measurements were made of the electric field profile of the dry resonant modes in the cavity of a TCP. The experiment remains to be completed and the single frequency technique developed during the preliminary testing has not yet been applied to plasmas in the TCP.

**I. INTRODUCTION**

This project is part of a larger effort to understand instabilities in plasmas. Plasma instabilities have already been studied in low-pressure inductive processing discharges with SF<sub>6</sub> and Ar/SF<sub>6</sub> mixtures<sup>1</sup>. Measurements were made of charged particle density, electron temperature and plasma potential using electrostatic probes and optical emission on a Transformer Coupled Plasma Source (TCP). Electron densities were measured with electrostatic probes. At low electron densities, the current to the probes is small so the relative error is large, and the probe measurements are of limited reliability. On the other hand, microwave cavity perturbation techniques are well suited to measuring low electron densities. This report investigates the use of cavity perturbation techniques to measure electron density in the low-density regime to supplement the data from the electrostatic probes.

Preliminary measurements were made on a mercury vapor discharge tube to assess the feasibility of various measurement systems. The discharge current was modulated to simulate an instability.

**II. THEORY**

The electron density  $n_e$  is measured by observing the frequency shift of a resonant mode of the cavity. For the test setup with the mercury vapor discharge tube, the TM<sub>010</sub> cylindrical cavity mode is used. For the TCP there are no clearly defined cylindrical cavity modes, because the ends of the chamber are partially covered with quartz plates rather than a conducting material, so an experimentally observed cavity mode is used instead.

To compute the electron density from the shift in resonant frequency we use Slater's perturbation formula:

---

<sup>1</sup> P Chabert, AJ Lichtenberg, MA Lieberman and A M Marakhtanov, "Instabilities in Low-Pressure Electronegative Discharges", submitted to Plasma Sources Science and Technology, December 2000.

$$\frac{\Delta\omega}{\omega_0} \approx \frac{1}{2\omega_0^2} \frac{\int \omega_p^2 |E|^2 dV_0}{\int |E|^2 dV_0}$$

where  $\Delta\omega$  is the shift in resonant frequency,  $\omega_0$  is the unperturbed resonant frequency,  $\omega_p$  is the (spatially varying) plasma frequency,  $E$  is the unperturbed resonance electric field, and the integral  $dV_0$  is over the total cavity volume. The electron density is then found from the plasma frequency, according to:

$$n_e = \omega_p^2 \left( \frac{\epsilon_0 m}{e^2} \right)$$

In this investigation the changes in resonant frequency are measured for a test setup with a mercury vapor discharge tube placed axially through a brass cylinder, and the corresponding electron densities are calculated. The remaining work, not completed in this investigation, is to perform similar measurements and calculations on the TCP and compare the results with the data from the electrostatic probe measurements.

### III. EXPERIMENTAL APPARATUS AND MEASUREMENTS

There were two main stages to the experiment. Firstly, measurements were made on a test setup with a mercury vapor discharge tube to assess the effectiveness of various measurement systems. Secondly measurements were made on the actual TCP.

#### Hg discharge setup

The experimental arrangement of the test setup is shown schematically in Figure 1. A Mercury vapor discharge tube is placed axially through a brass cylinder. The discharge tube itself is a glass cylinder of diameter approximately 1 cm, while the brass cylinder has an inside diameter of 12.02 cm and a length of 9.82 cm. The potential difference across the discharge tube is on the order of 500V. Each endplate of the cavity has a hole in the center through which the discharge tube is placed. One endplate has two additional holes along a diameter, through which microwave excitation and detection loops are placed. The loops are identical, 1 cm in diameter, with their planes lying along the endplate diameter. Resonances are excited by one loop, attached to a sweep oscillator. The resonance frequency is detected by the other loop, connected to a crystal diode detector. Based on the dimensions of the cylinder, the theoretical value of the  $TM_{010}$  resonance frequency is 1.9 GHz.

#### Swept frequency system on Hg discharge

Figure 2 shows a block diagram of the swept frequency system.

An HP 8350B Sweep Oscillator is used to excite a range of frequencies in the cavity. One sweep is performed every 17 ms. The sweep output of the oscillator gives a voltage proportional the frequency of the RF output, and is connected to the horizontal display on

the oscilloscope. The crystal detector is connected to the vertical display. When the excitation frequency matches the resonant frequency of the cavity, a peak is recorded on the oscilloscope display. Figures 3a and 3b show the trace obtained when the discharge is turned off. In this manner the dry resonance of the  $TM_{010}$  mode was determined to lie at 1.844 GHz. The slight discrepancy from the theoretical value of 1.9GHz is explained by the glass tube having a dielectric constant greater than unity, thereby decreasing the resonant frequency of the cavity.

The discharge current may be varied by altering the DC high voltage to the tube. When the current is increased, the electron density increases and the resonant frequency is observed to increase. This is attributable to the plasma having a dielectric constant of less than unity, according to the equation:

$$\epsilon_p = \epsilon_0 \left( 1 - \omega_p^2 / \omega^2 \right)$$

where  $\epsilon_p$  is the permittivity of the plasma,  $\omega_p$  is the plasma frequency and  $\omega$  is the driving frequency applied to the excitation loop. The ratio  $\epsilon_p / \epsilon_0$  is the dielectric constant.

Figure 4a shows a graph of the  $TM_{010}$  resonant frequency against discharge current and Figure 4b shows the electron density against current.

The nonlinear relationship between electron density and discharge current is due to the heating of the tube as the discharge current is increased. As the tube heats up, the mercury vapor pressure rises, further increasing electron density.

#### Raster display on Hg discharge

By placing an isolation transformer in series with the high voltage supply to the discharge tube, the discharge current was modulated at 60 Hz, with range 100 mA to 400 mA, to simulate an instability. An attempt was made to use a raster display so that the time variation of electron density could be followed. Figure 5 shows a block diagram of the raster display system.

In this system, the cavity was repeatedly swept over a moderate frequency interval on a time scale much faster than that of the current modulation. The fast time base, controlling the sweep, is on the order of 0.5ms. The slow time base is set to the period of the current modulation, 16.67ms. Hence there are approximately 30 raster lines in the display.

A typical display is shown in Figure 6. Note that two “waves” are visible. The right hand “wave” is the  $TM_{010}$  resonance as it changes with time. The left hand “wave” is a smaller amplitude mirror image of the resonance and is due to the sweep oscillator requiring a finite time to sweep the frequency downward. The HP 8350B Sweep Oscillator has an operating specification minimum sweep time of 10 ms, but in the raster system the fast time base is driving the oscillator with sweep time just 0.5ms. Given that the sweep oscillator is being used so far outside of its operating specifications, it is unsurprising that

an error is introduced by the finite time for a the downward sweep of frequency. Figure 7a shows the ideal form of the frequency output of the Sweep Oscillator against time, but based on the two waves visible in Figure 6 it may be inferred that the real form of frequency output against time is closer to that shown Figure 7b. If the HP8350B Sweep Oscillator were to be used within its operating specifications, with a sweep time of 10ms or greater, then the raster system could only be used to display modulations with frequencies at or below approximately 3 Hz.

Based in the above observations, it is apparent that the limitations of the HP 8350B oscilloscope render it impossible to obtain accurate measurements of resonant frequency with a discharge current modulation at 60 Hz. Since the actual plasma instabilities in the TCP have frequencies in the range of 1 to 10 kHz, the raster system is clearly unsuitable for measuring such instabilities.

### Single frequency system on Hg discharge

Given the unsuitability of the raster display, it was decided to use a single frequency measurement system. The block diagram for this system is shown in Figure 8.

A  $5\Omega$  resistor is placed in series with the discharge tube. The discharge current is modulated at 60 Hz, and its value is computed by measuring the voltage across the resistor. The sweep oscillator is set to some frequency  $f$  higher than the unperturbed  $TM_{010}$  frequency  $f_0$ . As the current modulates, the  $TM_{010}$  cavity resonance passes through  $f$  and a peak is recorded in the output of the crystal detector. Both the voltage across the resistor and the transmitted signal are displayed on the oscilloscope. A typical display is shown in Figure 9, with the RF frequency  $f$  set to 46 MHz higher than the unperturbed  $TM_{010}$  resonance frequency  $f_0$ . To determine the resonant frequency as a function of discharge current, measurements must be made for various values of  $f$ . The electron density can then be calculated from the resonant frequency. Figure 10a shows a graph of resonant frequency against current and Figure 10b shows a graph of electron density against current. Note that these graphs are linear, because over the 16.67 ms period of the current modulation, the temperature of the plasma does not change appreciably. Therefore the heating effect non-linearity discussed in the swept frequency section is not observed.

### TCP setup

The experimental arrangement of the TCP setup is shown schematically in Figure 11. The TCP cavity length is 19cm and the diameter is 30.25cm. The chamber walls are aluminum and the ends of the chamber are partially covered with quartz plates. Excitation and detection loops are placed through one end of the chamber in a similar fashion to the Hg discharge setup. The loops are identical, approximately 2cm in diameter, made of stainless steel wire, and are placed with their planes lying along an endplate diameter. The center of each loop is approximately 2.5 cm from the chamber wall. Resonances are excited by one loop, attached to a sweep oscillator. The resonance frequency is detected by the other loop, connected to a crystal diode detector. Based on the dimensions of the

cylinder, if it were to have conducting endplates then the theoretical value of the TM<sub>010</sub> resonance frequency is 760 MHz.

#### Measuring electric field of resonant modes in the TCP

The swept frequency system outlined earlier is used to determine the dry resonance modes of the TCP. Figure 12 shows an oscilloscope trace of the resonance modes. The electric field profiles of several of the modes are determined by measuring their frequency shifts versus the position of a small dielectric sphere. The sphere is 35mm in diameter, made of Teflon, and held on a cylindrical ceramic stem of radius 3mm. The sphere is moved along a diameter 22.5° from the loops, approximately 4cm from the endplate opposite the loops.

The small amplitude resonant modes at 264 MHz, 508 MHz, and 1.16 GHz exhibit very little dependence on the position of the sphere. The modes at 1.55GHz, 1.70GHz, 1.75GHz, 1.81GHz and 1.99GHz all exhibit some dependence on the position of the sphere, and the shifts in the frequencies of these modes versus the position of the sphere are shown in Figures 13a, 13b, 13c, 13d and 13e respectively. The frequency shift is measured relative the case with the sphere absent from the chamber. Note that the shift is always negative, since the sphere has a dielectric constant of greater than unity. According to electromagnetic theory the absolute magnitude of the frequency shift is proportional to the square of the electric field magnitude at the position of the sphere, so these graphs effectively show the radial variation of the square of the electric field magnitude of the various resonant modes.

At 1.45GHz and 1.61GHz there are sharp dips in the transmitted signal, and the frequencies at which these dips occur are observed to depend on the position of the sphere. Figures 14a and 14b show oscilloscope traces of these dips, while Figures 15a and 15b show the shifts in the frequencies of the dips versus the position of the sphere.

#### **IV CONCLUSION**

Microwave cavity perturbation techniques have been studied with the chamber of a Transformer Coupled Plasma source and with a mercury vapor discharge tube plasma on the axis of a smaller cavity. The aim of these investigations was to develop a method of measuring the electron density  $n_e$  in unstable, low-pressure, inductive processing discharges. Testing on the mercury vapor discharge setup revealed that the implementation of a raster display using an HP8350B Sweep Oscillator leads to inaccurate results if the perturbation modulates with a frequency on the order of 60Hz or greater. An alternative, single frequency method was proposed and shown to be effective in measuring a modulation at 60Hz in the mercury vapor discharge setup. An interesting side result of the work carried out on the mercury vapor discharge setup was that the electron density in the discharge tube varies linearly with the discharge current if the discharge current is AC, but nonlinearly if the discharge current is DC. The nonlinearity in the latter case was explained by the heating of the discharge tube at higher currents leading to a greater mercury vapor pressure. Work performed on the TCP included measurements of the resonant frequencies, and the shifts in the resonant frequencies versus the position of a small dielectric sphere. From these measurements one can



determine the radial variation of the electric field magnitude for the various modes. These electric field profiles are necessary in order to perform the integrals in Slater's perturbation formula. It remains to apply the single frequency technique, developed during testing on the mercury vapor discharge setup, to plasmas in the TCP.

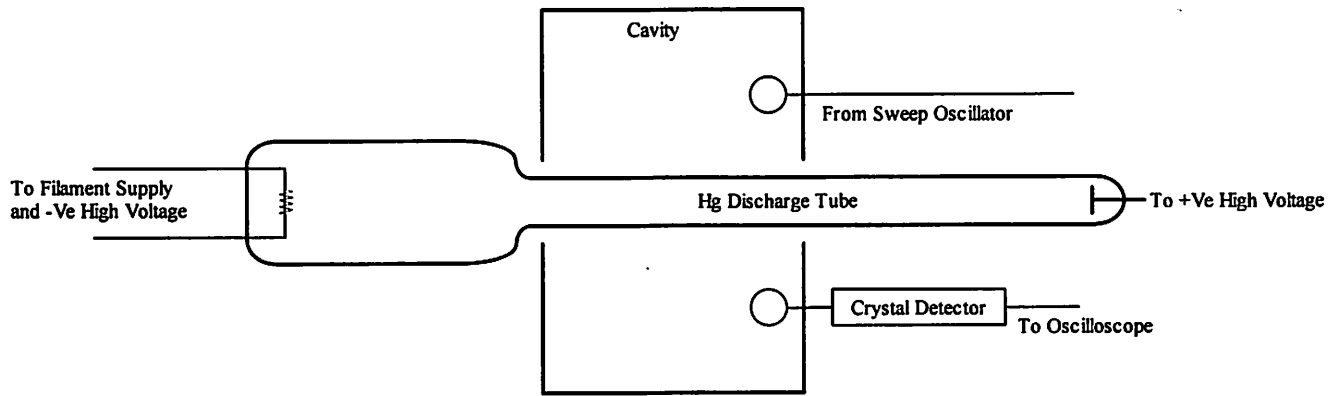


**Figure 1. Schematic diagram of Hg discharge tube in brass cavity.**

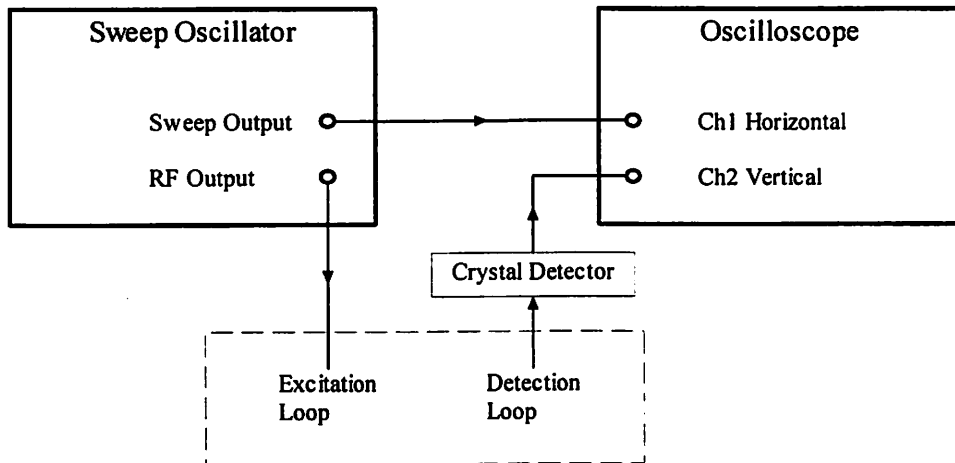


**Figure 2. Block diagram of the swept frequency system used to measure the  $TM_{010}$  resonance.**

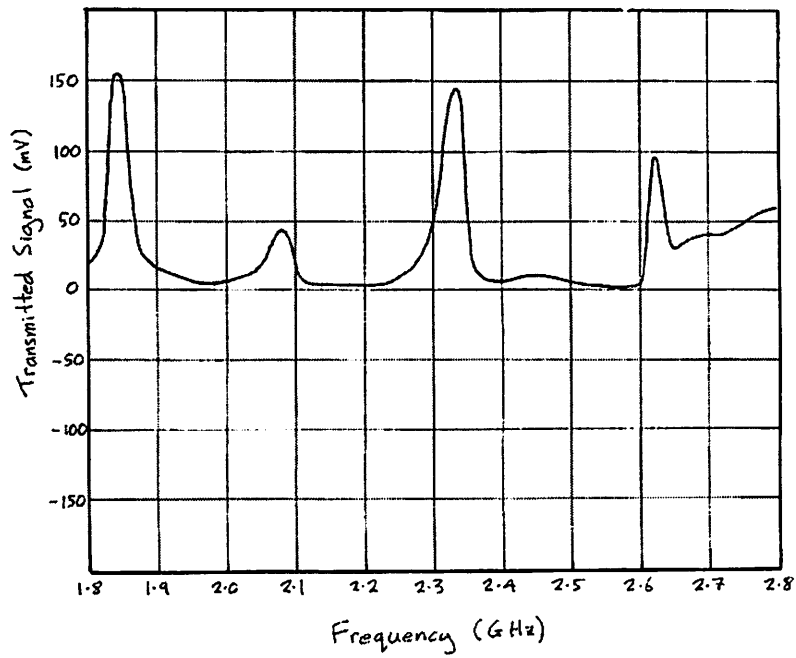


**Figure 3a. From left to right, oscilloscope display of the  $TM_{010}$ ,  $TM_{111}$ ,  $TM_{011}$  and  $TM_{211}$  resonances, with plasma absent.**

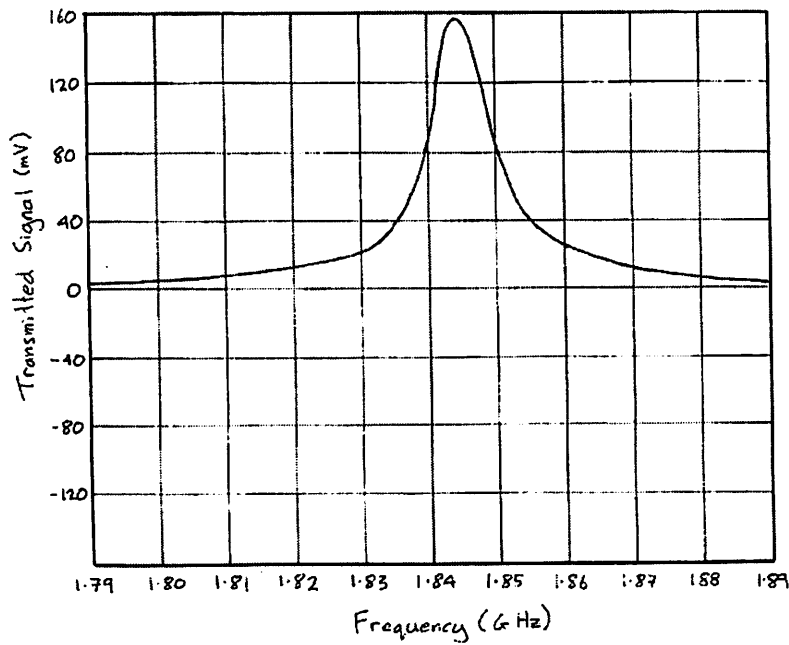


**Figure 3b. Oscilloscope display of the  $TM_{010}$  resonance, with plasma absent**

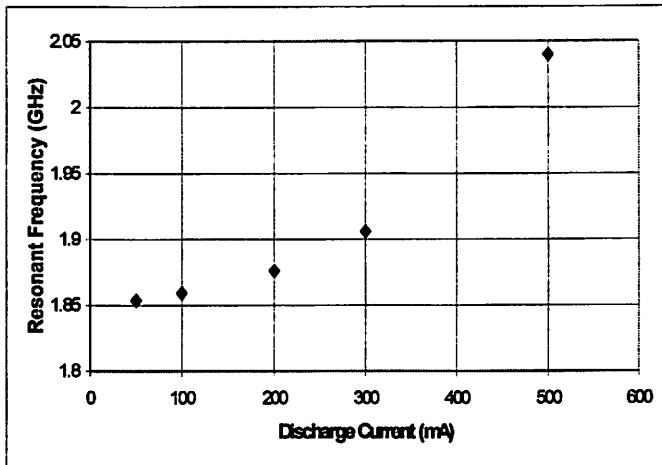


**Figure 4a.  $TM_{010}$  resonant frequency as a function of DC discharge current.**

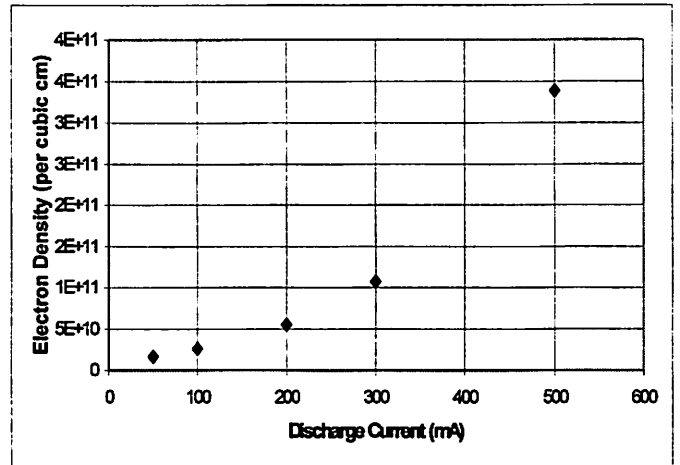


**Figure 4b. Electron density as a function of DC discharge current.**

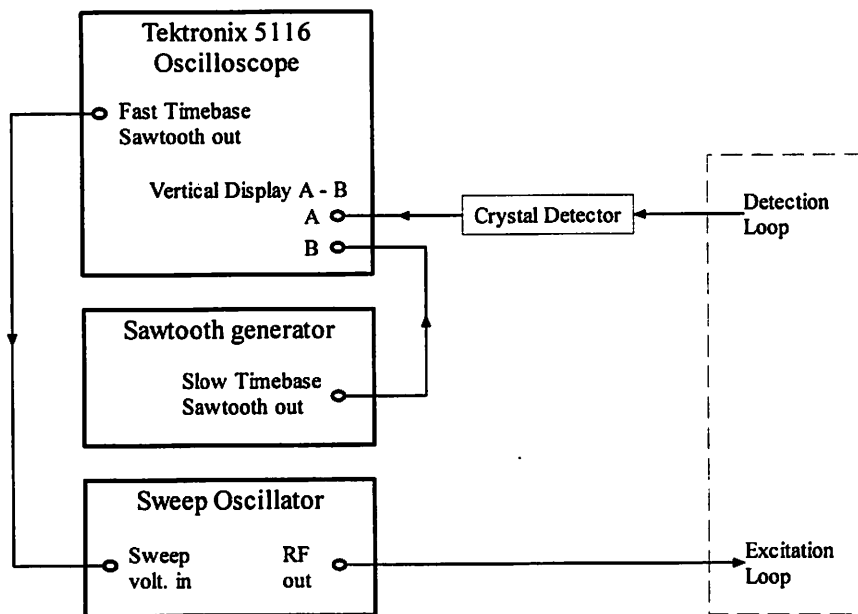


**Figure 5. Block diagram of the swept-frequency system used to measure the time variation of the  $TM_{010}$  mode shift.**

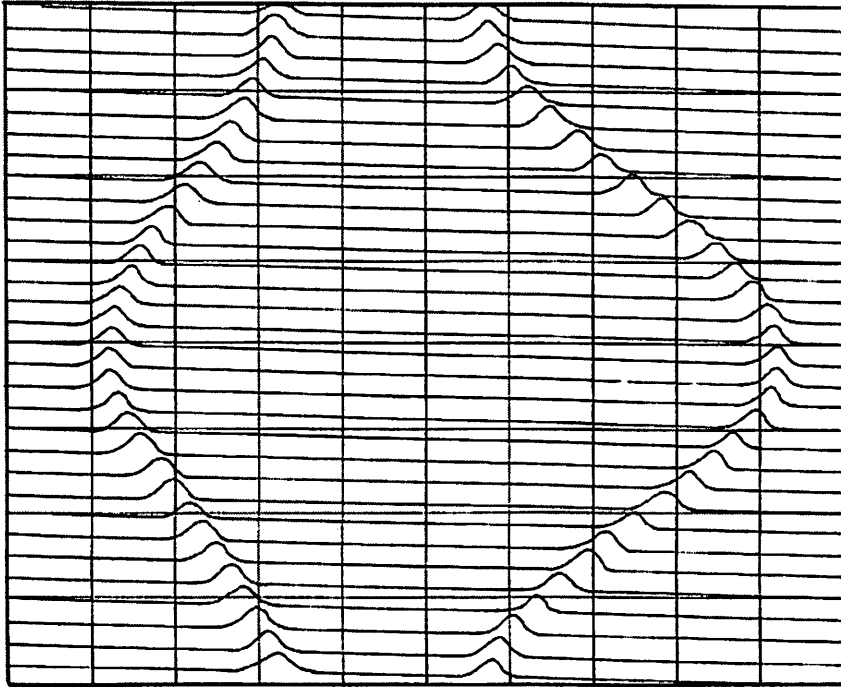


**Figure 6. Raster display of the cavity signal, showing the time variation of the TM010 mode as the discharge current is modulated. The horizontal time scale is 0.050ms/div and the vertical timescale is 2.08ms/div.**

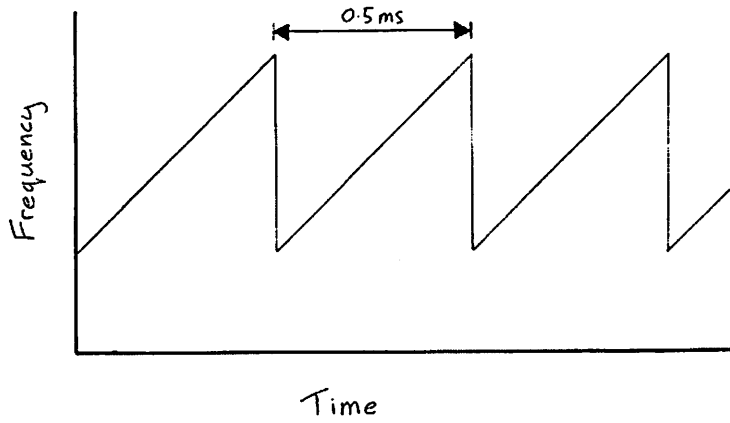


**Figure 7a. Ideal form of the time variation of RF output frequency of sweep oscillator.**

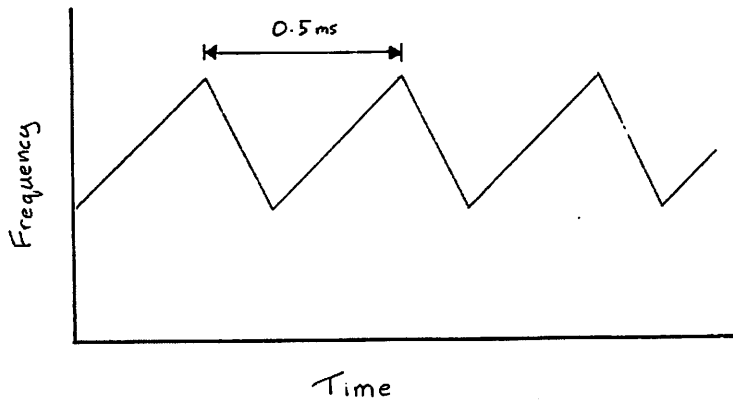


**Figure 7b. Inferred actual form of time variation of RF output frequency of sweep oscillator.**



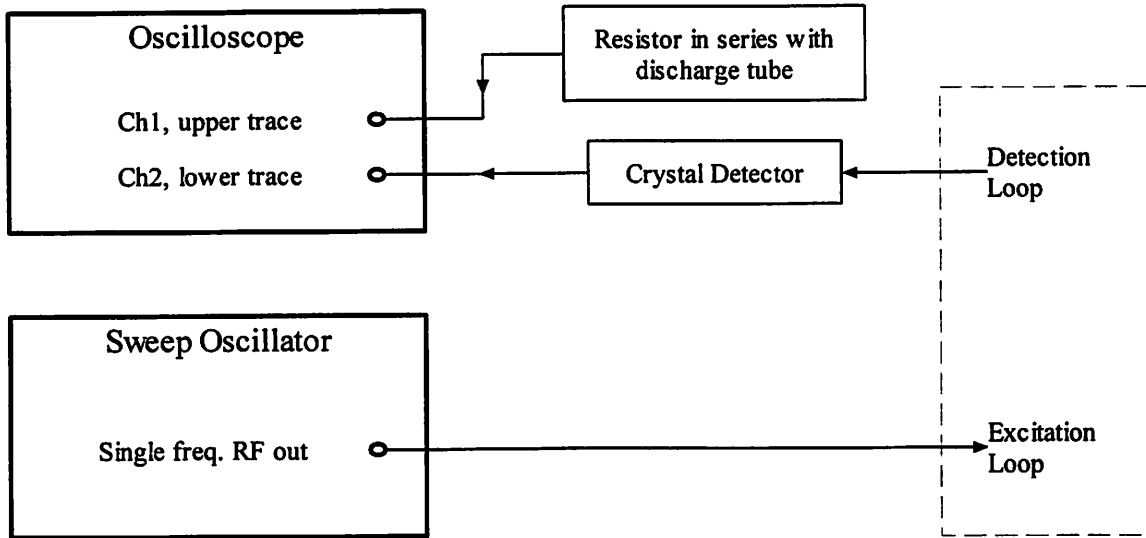


**Figure 8. Block Diagram of the single frequency system used to measure the  $TM_{010}$  shift.**

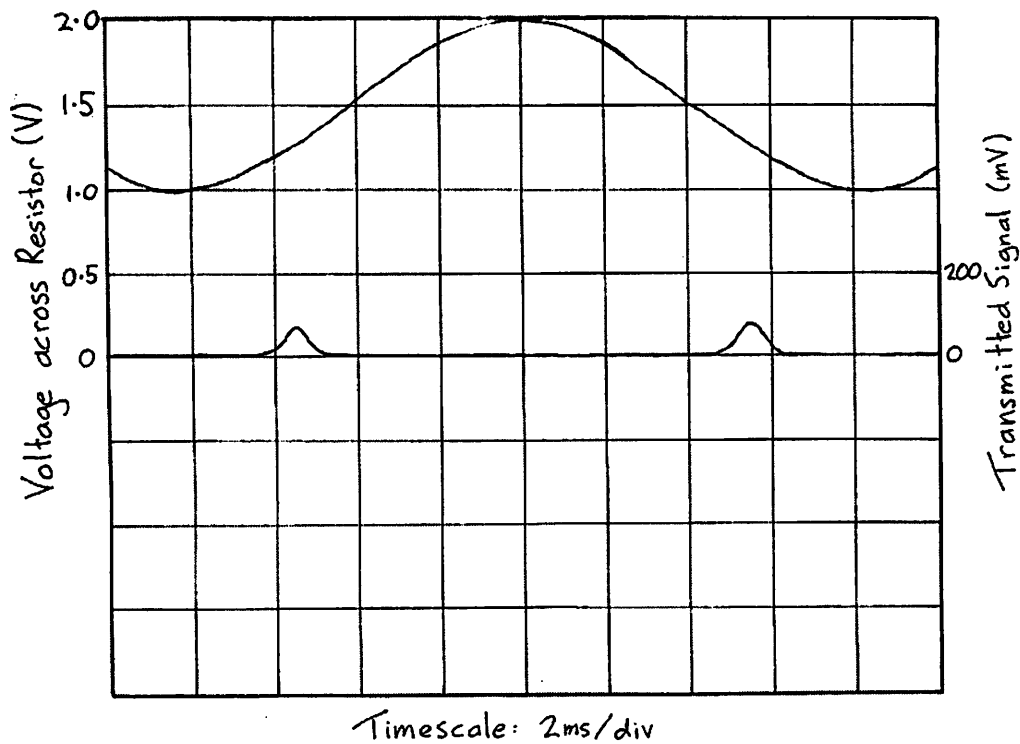


**Figure 9. Typical oscilloscope display for the single frequency method used to measure the TM010 shift, in this case with  $(f-f_0) = 46$  MHz. Upper trace: voltage across resistor. Lower trace: cavity transmission signal.**

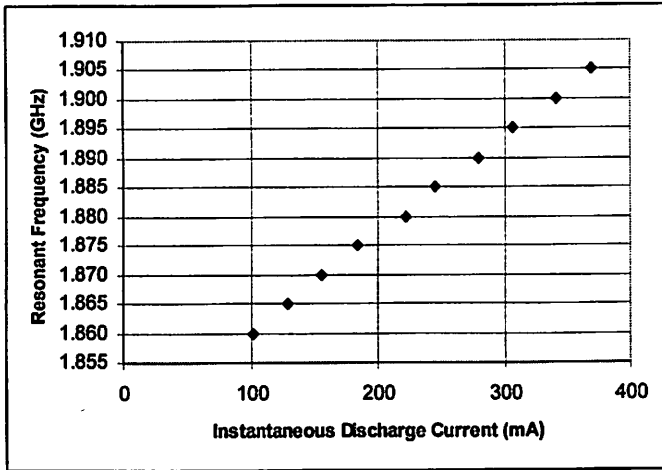


**Figure 10a.  $TM_{010}$  resonant frequency as a function of AC discharge current.**

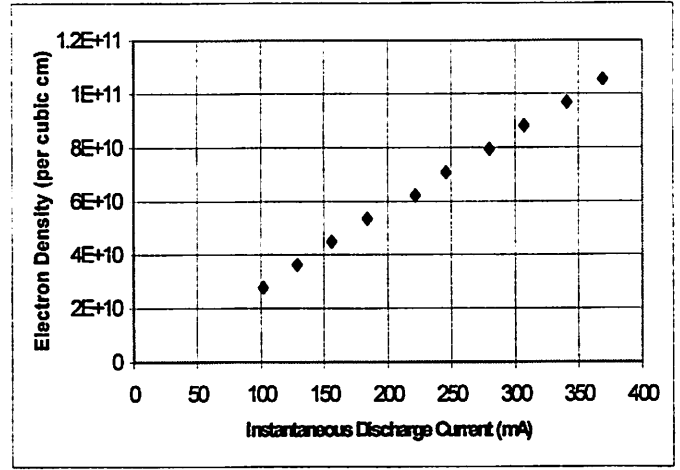


**Figure 10b. Electron density as a function of AC discharge current.**

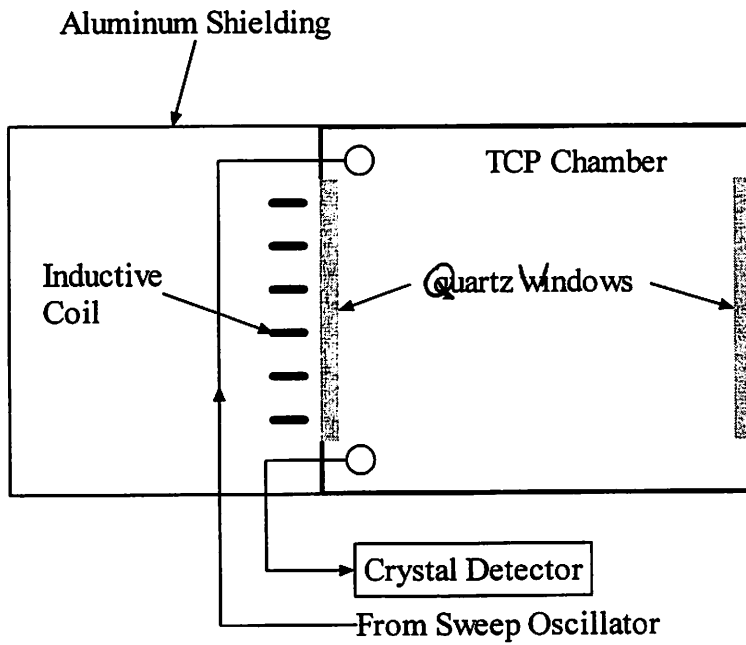


**Figure 11. Schematic diagram of the Transformer Coupled Plasma Source**

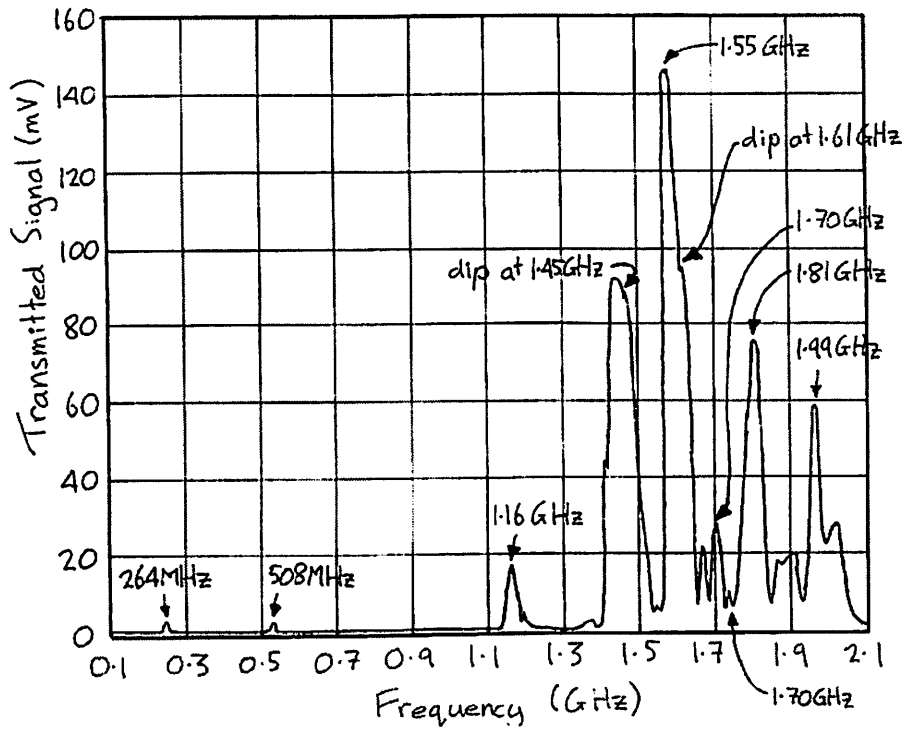


**Figure 12. The resonant modes of the TCP chamber without plasma.**

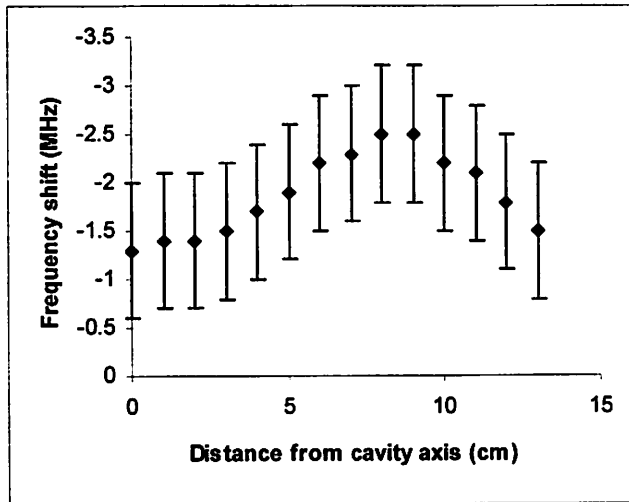


**Figure 13a. Frequency shift versus dielectric sphere position for the resonance at approximately 1.55GHz.**

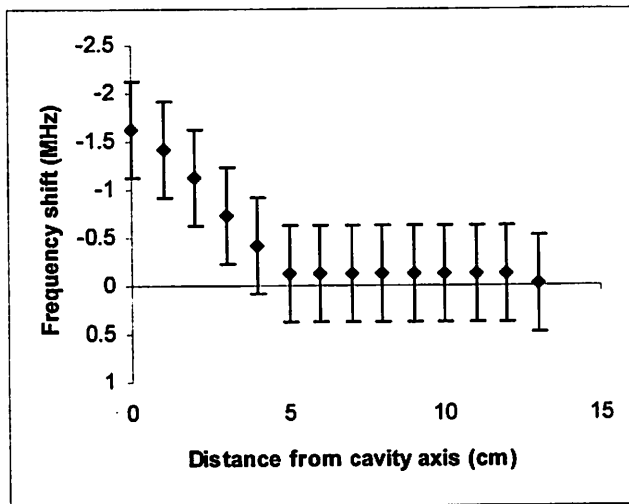


**Figure 13b. Frequency shift versus dielectric sphere position for the resonance at approximately 1.70GHz.**

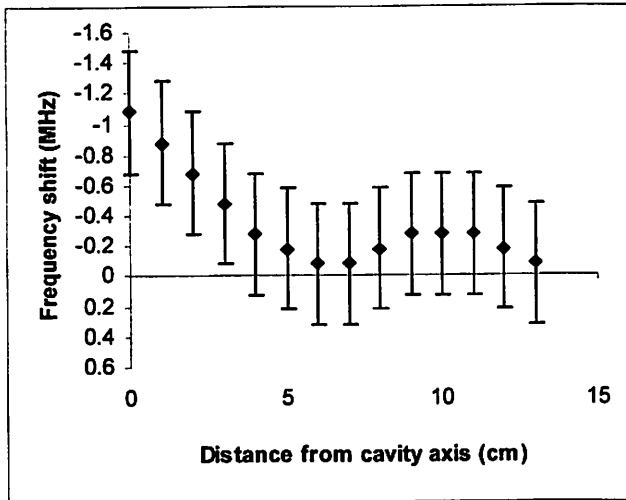


**Figure 13c. Frequency shift versus dielectric sphere position for the resonance at approximately 1.75 GHz.**

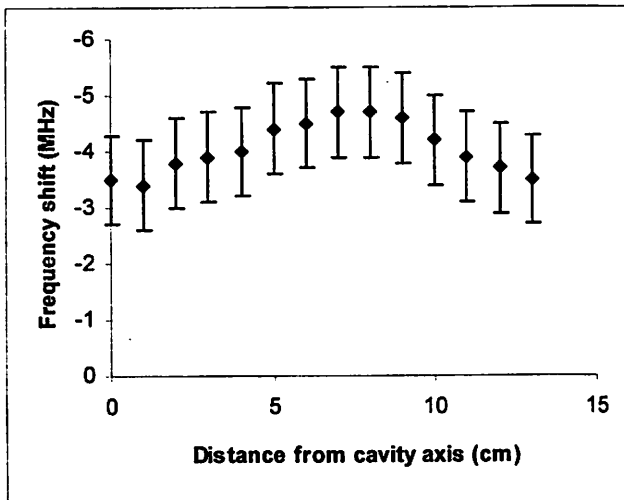


**Figure 13d. Frequency shift versus dielectric sphere position for the resonance at approximately 1.81 GHz.**

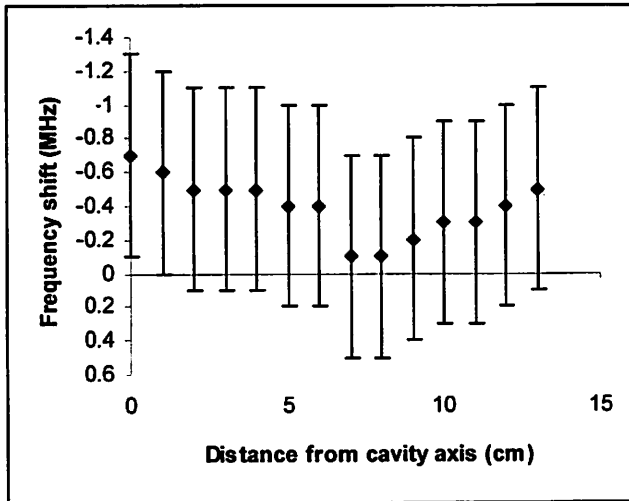


**Figure 13e. Frequency shift versus dielectric sphere position for the resonance at approximately 1.99 GHz.**



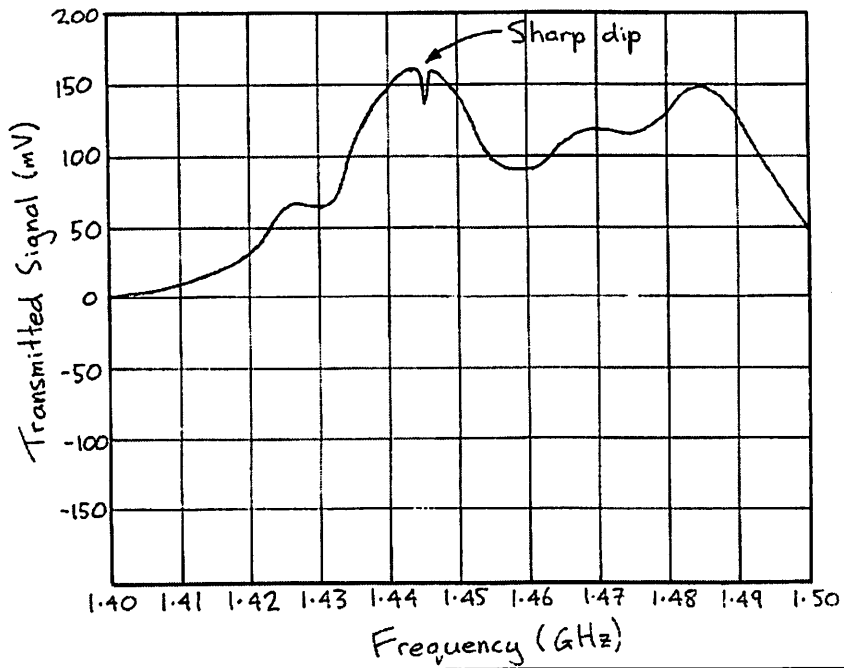


**Figure 14a. Oscilloscope trace of the dip in the transmitted signal at approximately 1.45 GHz, with the dielectric sphere absent.**

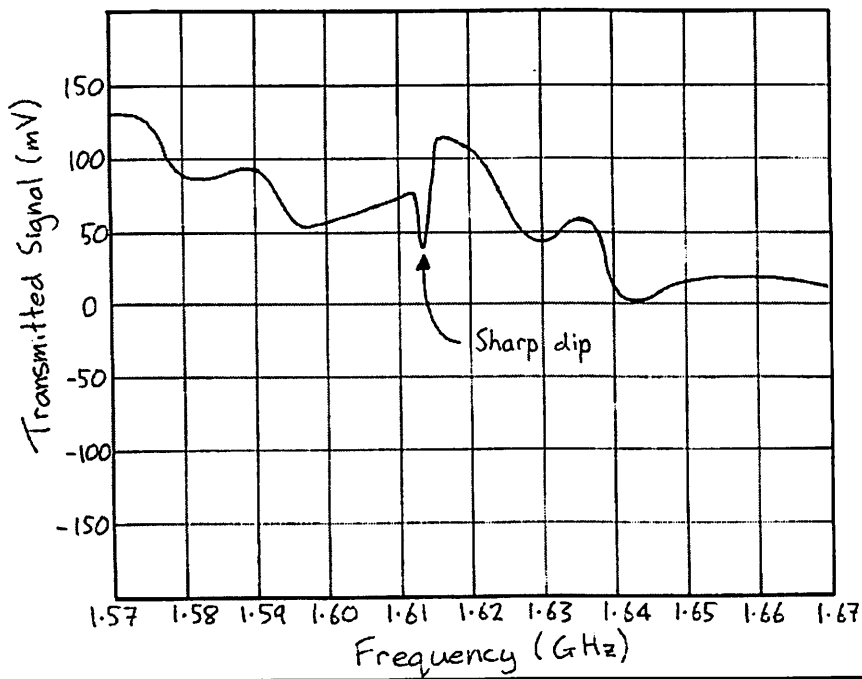


**Figure 14b. Oscilloscope trace of the dip in the transmitted signal at approximately 1.61 GHz, with the dielectric sphere absent.**

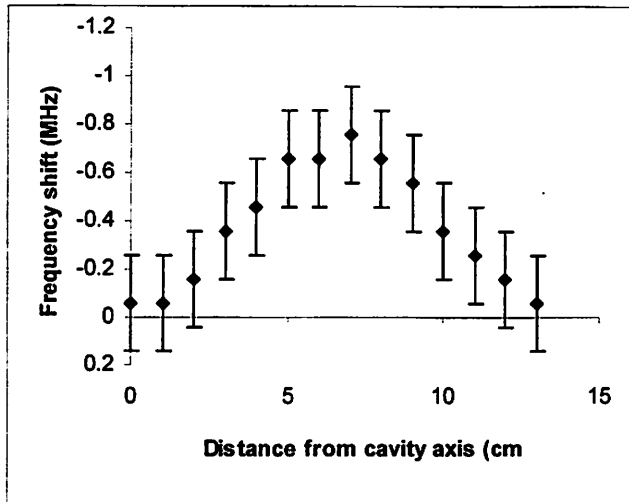


**Figure 15a. Magnitude of frequency shift versus dielectric sphere position for the dip in the transmitted signal at approximately 1.44GHz.**

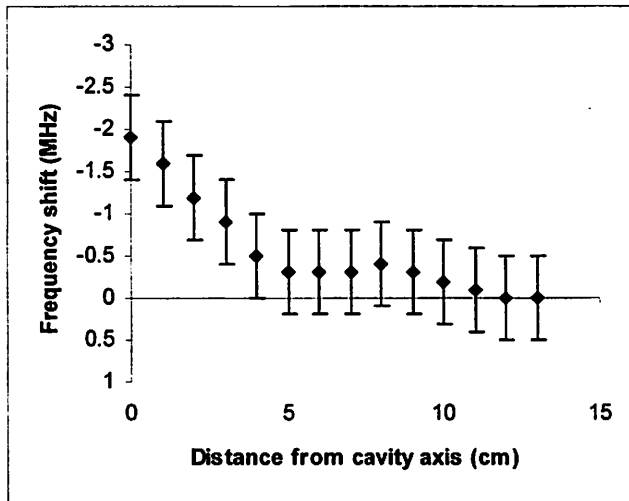


**Figure 15b. Magnitude of frequency shift versus dielectric sphere position for the dip in the transmitted signal at approximately 1.61GHz.**